Progress in development of soft X-ray two-filter diagnostic for electron temperature measurement in VEST

M. W. Lee [a], Soobin Lim [b], Wonik Jung [b], Y. S. Hwang [b], C. Sung [a*]
[a]*Department of Nuclear and Quantum Engineering, Korea Advanced Institute of Science and Technology, Daejeon 34141, Republic of Korea*
[b]*Department of Energy Systems Engineering, Seoul National University, Seoul 08826, Republic of Korea*
[*]*Corresponding author: choongkisung@kaist.ac.kr*

1. Introduction

Soft X-ray (SXR) diagnostics have been widely used in the study of the magnetohydrodynamic activities of fusion plasma [1,2], due to their fast time resolution and non-invasive measurement. In the versatile experiment spherical torus (VEST) [3], a 40-channel SXR camera system has been installed [4] to get two-dimensional SXR images through tomographic reconstruction [5]. In addition to this system, we are developing another SXR system for electron temperature (T_e) measurement. Although SXR intensity is a function of multiple plasma parameters such as electron density (n_e), temperature, and effective ion charge ($Z_{eff}=\sum_j Z_j^2 n_j/Z_j n_j$, j is ion species), we can estimate line-integrated T_e along the lines-of-sight (LOS) through a two-filter method [6]. Moreover, local profiles of T_e can be obtained through tomography of multi-channel SXR measurement with the two-filter method. In this paper, we report the progress in the development of a two-filter SXR diagnostic in VEST.

2. Methods and Results

2.1 Two-filter Method

The two-filter method estimates electron temperature by comparing the ratio of SXR signal through two different filters coming from the same LOS in the plasma. In the plasma, SXR emissivity from bremsstrahlung continuum is a convolution of plasma parameters such as Z_{eff}, n_e, and T_e. Therefore, the emissivity P_{rad} through certain filter of transmittance, eff(E), is given by [7]

$$P_{rad} = C \cdot \int \frac{n_e^2 Z_{eff}}{\sqrt{T_e}} e^{-\frac{E}{T_e}} \mathrm{eff}(E) dE \quad (1)$$

Here, the constant C includes the gaunt factor and geometrical factors, and E is the energy of the photon. Equation (1) can be rewritten to highlight its dependency on the T_e,

$$P_{rad} = C^* \cdot \int \frac{1}{\sqrt{T_e}} e^{-\frac{E}{T_e}} \mathrm{eff}(E) dE \quad (2)$$

where $C^* = C n_e^2 Z_{eff}$ since Z_{eff} and n_e are not affected by photon energy, E. By dividing the two signals with two different filters, we can get a function depending on the T_e.

$$R(T_e) = \frac{\int e^{-\frac{E}{T_e}} eff_1(E) dE}{\int e^{-\frac{E}{T_e}} eff_2(E) dE} \quad (3)$$

Equation (3) is a monotonic function to a certain temperature, indicating T_e can be obtained by measuring the ratio of SXR intensity with two different filters. The shape of the ratio-temperature curve obtained from Eq. (3) varies with filter combination, so it is important to select a proper filter set by application. Considering the estimated temperature of VEST Ohmic discharge, we selected aluminum (Al) 1.0 um and silver (Ag) 0.2 um as the initial filter set. Fig. 1(a) shows the transmission curves of the Al and Ag filters. The possible measurement range is about 30 eV–140 eV, as shown in Fig. 1(b), which is calculated using Eq. (3).

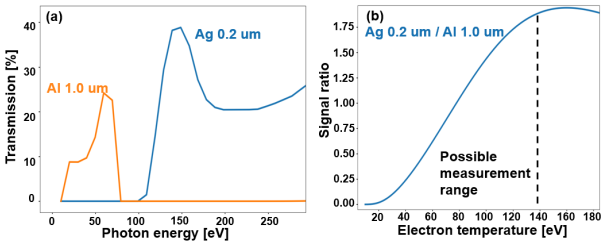

Fig. 1 (a) Transmission curve of Ag 0.2 um and Al 1.0 um filters. (b) Ratio-temperature curve of the Ag and Al filter set.

2.2 Soft X-ray Measurement System

To measure SXR, a pinhole camera capable of mounting multiple filters was designed. Fig. 2 shows the interior design of the SXR camera. 16-channel absolute extreme-UV (AXUV) photodiode array was used as the SXR sensor, and two AXUVs were placed 4 cm apart in the toroidal direction of the torus, as shown in Fig. 2(a). Therefore, the camera has 32 channels with two AXUVs, and 16 LOS in a poloidal plane. Then, light covers were located on the AXUV to prevent possible stray light. A filter wheel, which can mount six filters, was utilized to test various filters and pinhole sizes without breaking the vacuum. The filter wheel is connected to the rotary wheel, which is rotatable outside the vacuum. Specifically, we installed a preamp inside the camera to reduce noise by shortening the connection between the sensor and the preamp. As shown in Fig. 2(b), the custom preamp board is directly inserted at the bottom of AXUV and then connected to the feedthrough without a cable. As for the preamp, we applied a 32-channel preamp with a transimpedance gain of 10^6 V/A. Finally, we put a stainless-steel shield onto the camera, as shown in Fig. 2(c). The SXR camera was then installed in the upper part of the VEST.

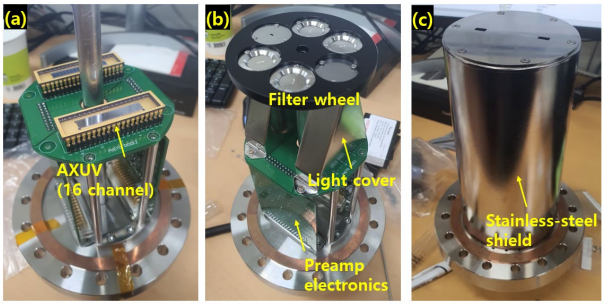

Fig. 2 (a) Interior of the pinhole camera. Two AXUV 16 were used. (b) Filter wheel and light cover were installed along the light path, and the preamp electronics were directly connected to AXUV and feedthrough. (c) The complete pinhole camera with a stainless-steel shield.

The amplified signal is transmitted to the outside of the vacuum through a D-sub cable bundle. The cable bundle is connected to a power supply for the preamp, and we used a 24V battery to minimize noise by isolating the power line of the VEST chamber. Then, the signal goes to the digitizer (CAEN VME 8008X, maximum 125 MHz sampling) and is eventually stored in the data acquisition system.

2.3 Preliminary Results from VEST Discharge

We tested the camera in the VEST Ohmic discharge (shot #38269). Figure 3(a) shows the LOS of SXR measurements, and Figure 3(b) presents multi-channel measurement results from Al 1.0 um filter. The maximum plasma current (I_p) in the discharge was approximately 100 kA, as shown in Fig. 3(c).

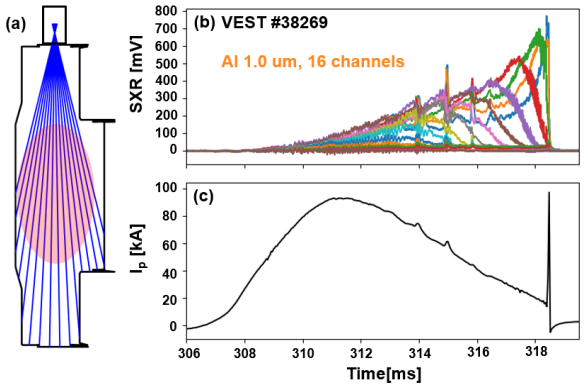

Fig. 3. Schematics of installed system and signal time trace during VEST discharge #38269. (a) The system has 16-LOS in a poloidal plane to cover entire plasma. (b) 16-channel signal from Al 1.0 um filter. (c) I_p time trace.

A high-quality signal without offset and noise is important for the signal ratio. In these measurements, the different offset levels existed in each channel, mainly because of the leakage current of each semiconductor channel of AXUV. To eliminate the offset, we averaged the signal before plasma formation and subtracted it from the measured signal. As shown in Fig. 3(b), we could effectively adjust each offset level by this method. Moreover, Fourier spectrum of the signal showed no significant noise under 200 kHz. Because the plasma spectrum in VEST, which got from magnetic coils, is usually under 100 kHz, we applied an additional 100 kHz digital low-pass filter to minimize the high-frequency noise.

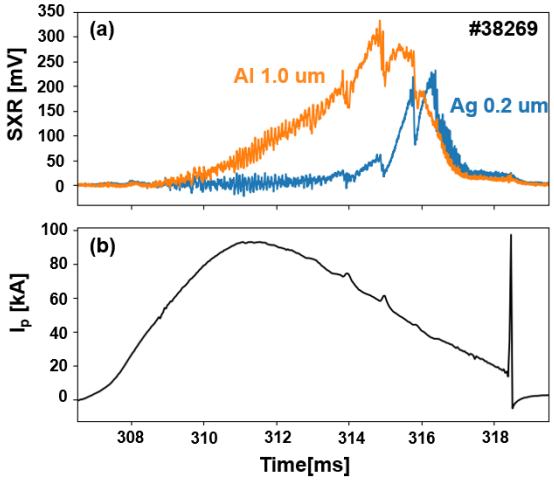

Fig. 4. (a) SXR signal from a core sight line through Al 1.0 um and Ag 0.2 um filters. (b) I_p time trace.

From the test with the filter combination using Al and Ag, we observed that the signal level from the Ag filter was considerably low, especially in the I_p ramp-up phase (308 ms–311 ms), as shown in Fig. 4(a). The fluctuations observed during the ramp-up phase had a root-mean-square amplitude of 14 mV with the frequency of 11 kHz. However, the mean value of 10 kHz low-pass filtered Ag signal during this phase was under 10 mV, even with the pinhole size of 1×4 mm^2, which was the maximum size we tested. The current Ag filter was supposed to cut off the photon under 100 eV, as shown in Fig. 1(b), so this low signal level means that the number of photons above 100 eV emitted from the plasma was quite small in the early stage of the Ohmic discharge scenario.

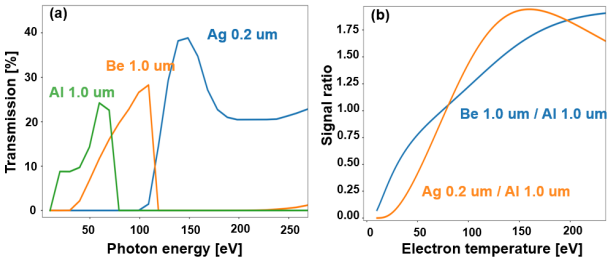

Fig. 5. (a) Transmission of Al 1.0 um and Ag 0.2 um, and Be 1.0 um filters. (b) Ratio-temperature curves of the filter sets.

The insufficient signal level of 0.2 um Ag-filtered channels makes it difficult to determine the signal ratio between the two channels. Therefore, to precisely measure the electron temperature, including I_p ramp-up phase, it is necessary to maximize the signal level from the Ag filter. The current Ag filter can be manufactured with a minimum thickness of 0.1 um, and in this case, the signal is expected to be doubled as the transmittance increases. In addition to the thinner Ag filter, beryllium

(Be) has transmittance in the intermediate energy band between Al and Ag, shown in Fig. 5(a). From the ratio-temperature curve in Fig. 5(b), Be 1.0 um filter is expected to show a signal level of about 80% of Al at 50 eV plasma. We will further investigate the different filter sets to get proper ratio estimation in future work.

3. Conclusions

We developed a multi-channel SXR camera system that can apply the two-filter method and installed the system on VEST. For the filter set, we selected a combination of Al and Ag filters with different transmission bands. The initial measurements showed that multi-channel measurements using a 1.0um Al filter were possible without significant noise level. However, the level of the 0.2 um Ag filtered signal was similar to the background noise level and much smaller than that of the Al-filtered signal in the I_p ramp-up phase. Thus, additional optimization of filter selection is required to apply the two-filter method. We will apply a thinner Ag filter first. In addition, we plan to attempt a Be filter that shows transmittance in the energy band between 50–100 eV to increase the signal level.

Acknowledgments

This research was supported by the National R & D Program through the National Research Foundation of Korea (NRF) funded by the Ministry of Science and ICT (2021M3F7A1084418).

REFERENCES

[1] C. Brandt et al., Soft x-ray tomography measurements in the Wendelstein 7-X stellarator, Plasma Phys. Control. Fusion. 62 (2020) 035010. https://doi.org/10.1088/1361-6587/ab630d.
[2] L. Delgado-Aparicio et al., Soft x-ray measurements of resistive wall mode behavior in NSTX, Plasma Phys. Control. Fusion. 53 (2011) 035005. https://doi.org/10.1088/0741-3335/53/3/035005.
[3] K.J. Chung, Y.H. An, B.K. Jung, H.Y. Lee, C. Sung, Y.S. Na, T.S. Hahm, Y.S. Hwang, Design Features and Commissioning of the Versatile Experiment Spherical Torus (VEST) at Seoul National University, Plasma Sci. Technol. 15 (2013) 244–251. https://doi.org/10.1088/1009-0630/15/3/11.
[4] J.Y. Jang, S. Lim, S. Kim, M.W. Lee, Y.-G. Kim, C. Sung, Y.S. Hwang, Development of a soft x-ray (SXR) array diagnostic system on versatile experiment spherical torus (VEST), Review of Scientific Instruments. 93 (2022) 093506. https://doi.org/10.1063/5.0101883.
[5] J. Schilling, H. Thomsen, C. Brandt, S. Kwak, J. Svensson, Soft x-ray tomograms are consistent with the magneto-hydrodynamic equilibrium in the Wendelstein 7-X stellarator, Plasma Phys. Control. Fusion. 63 (2021) 055010. https://doi.org/10.1088/1361-6587/abe0fa.
[6] P. Franz, F. Bonomo, L. Marrelli, P. Martin, P. Piovesan, G. Spizzo, B.E. Chapman, D. Craig, D.J. Den Hartog, J.A. Goetz, R. O'Connell, S.C. Prager, M. Reyfman, J.S. Sarff, Two-dimensional time resolved measurements of the electron temperature in MST, Review of Scientific Instruments. 77 (2006) 10F318. https://doi.org/10.1063/1.2229192.
[7] T. Bando, S. Ohdachi, Y. Suzuki, Developments of scintillator-based soft x-ray diagnostic in LHD with CsI:Tl and P47 scintillators, Rev. Sci. Instrum. 87 (2016) 11E317. https://doi.org/10.1063/1.4960418.